● RESEARCH ARTICLE

Glial fibrillary acidic protein levels are associated with global histone H4 acetylation after spinal cord injury in rats

Mayara Ferraz de Menezes[1, 2], Fabrício Nicola[3], Ivy Reichert Vital da Silva[4], Adriana Vizuete[3], Viviane Rostirola Elsner[4, *], Léder Leal Xavier[1, 2], Carlos Alberto Saraiva Gonçalves[3], Carlos Alexandre Netto[3], Régis Gemerasca Mestriner[1, 2]

1 Neurorehabilitation and Neural Repair Research Group, Pontifícia Universidade Católica do Rio Grande do Sul, Porto Alegre, RS, Brazil
2 Graduate Program in Cellular and Molecular Biology, Pontifícia Universidade Católica do Rio Grande do Sul, Porto Alegre, RS, Brazil
3 Department of Biochemistry, Basic Science Institute, Universidade Federal do Rio Grande do Sul, Porto Alegre, RS, Brazil
4 Graduate Program in Biosciences and Rehabilitation. Centro Universitário Metodista IPA, Porto Alegre, RS, Brazil

Abstract

Emerging evidence has suggested global histone H4 acetylation status plays an important role in neural plasticity. For instance, the imbalance of this epigenetic marker has been hypothesized as a key factor for the development and progression of several neurological diseases. Likewise, astrocytic reactivity - a well-known process that markedly influences the tissue remodeling after a central nervous system injury - is crucial for tissue remodeling after spinal cord injury (SCI). However, the linkage between the above-mentioned mechanisms after SCI remains poorly understood. We sought to investigate the relation between both glial fibrillary acidic protein (GFAP) and S100 calcium-binding protein B (S100B) (astrocytic reactivity classical markers) and global histone H4 acetylation levels. Sixty-one male Wistar rats (aged ~3 months) were divided into the following groups: sham; 6 hours post-SCI; 24 hours post-SCI; 48 hours post-SCI; 72 hours post-SCI; and 7 days post-SCI. The results suggested that GFAP, but not S100B was associated with global histone H4 acetylation levels. Moreover, global histone H4 acetylation levels exhibited a complex pattern after SCI, encompassing at least three clearly defined phases (first phase: no changes in the 6, 24 and 48 hours post-SCI groups; second phase: increased levels in the 72 hours post-SCI group; and a third phase: return to levels similar to control in the 7 days post-SCI group). Overall, these findings suggest global H4 acetylation levels exhibit distinct patterns of expression during the first week post-SCI, which may be associated with GFAP levels in the perilesional tissue. Current data encourage studies using H4 acetylation as a possible biomarker for tissue remodeling after spinal cord injury.

Key Words: histones; spinal cord injury; glial fibrillary acidic protein; S100 calcium-binding protein B; neural plasticity; astrocyte; ELISA-immunoassay; recovery; neural repair; rats

Introduction

Spinal cord injury (SCI) is an important cause of disability in adults, imposing a significant economic burden worldwide (Silva et al., 2014). Traumatic events, such as car accidents, falls and urban violence are among the main causes of SCI (Lee et al., 2011; Oyinbo, 2011; Silva et al., 2014).

For many years, researchers have worked to develop neuroprotective strategies, mostly focused on neurons or the neurovascular unit (Abeysinghe et al., 2016; Wu et al., 2016). However, the modulation of molecular cascades after central nervous system (CNS) injuries, such as SCI, is still a matter of debate since preclinical findings have not yet been successfully translated from the bench to the bedside (Maki et al., 2013; Tasker and Duncan, 2015). This is critical because an understanding of injury-induced plasticity usually provides insights into new therapeutic targets (Tasker and Duncan, 2015).

Epigenetic modifications have been shown to be influenced by gene-environment interactions, which change neural cell activity through gene transcription and silencing (Di Giammartino and Apostolou, 2016; Maleszka, 2016), affecting neuroplasticity (Kim et al., 2012; Vogel-Ciernia

et al., 2013). For instance, histone-modifying enzymes can remodel the chromatin structure indirectly by regulating the expression of injury-induced genes (Finelli et al., 2013; Wong and Zou, 2014). The histone acetylation status is regulated by histone acetyltransferases and histone deacetylases (HDAC) enzymes, which add and remove acetyl groups to N-terminal histone tails, respectively, thus inducing short or long-term chromatin architecture modulation (Arrowsmith et al., 2012; Park et al., 2016; Watson and Tsai, 2017). Moreover, the imbalance in these enzyme activities is related to the development of several neurological disorders (Saha and Pahan, 2006; Finelli et al., 2013; Park et al., 2016).

Previous reports have suggested epigenetic modulation could influence axon growth potential as well as the properties of remaining tissue after SCI (Yu et al., 2009; Finelli et al., 2013; Wong and Zou, 2014; Kim et al., 2016; Maleszka, 2016). Additionally, several studies have associated global histone H4 acetylation levels with normal and pathological development of the CNS. For example, histone H4 acetylation levels may become hyperacetylated in Parkinson's disease (Jin et al., 2014), Huntington's chorea (Saha and Pahan, 2006) and Friedreich's ataxia (Herman et al., 2006). By

contrast, changes in H4 acetylation play a fundamental role in synaptogenesis, synaptic plasticity, learning and memory (Kim et al., 2012; Vogel-Ciernia et al., 2013; Watson and Tsai, 2017). Nonetheless, the global histone H4 acetylation status in the perilesional tissue after SCI remains unclear. Thus, identifying the profile of global H4 acetylation levels after SCI could be an important step to establish a therapeutic window for epigenetic interventions.

Remodeling neural tissue after injury – a graded and multi-stage process involving various molecular and morphological changes – has been described as an evolutionary conserved defensive key factor for neural repair and plasticity (Burda and Sofroniew, 2014; Sofroniew, 2015). However, this process has a dual role in neurotrauma (Pekny et al., 2014). On the one hand, it plays an essential role in isolating injured spinal cord tissue (*i.e.*, cystic cavity and the isolation of surrounding cells) and triggering neuroprotective mechanisms (Pekny and Pekna, 2014; Pekny et al., 2014; Sofroniew, 2015; Abeysinghe et al., 2016). On the other hand, an exaggerated adaptive response can inhibit plasticity and repair processes such as axonal rewiring and neuronal sprouting (Pekny and Pekna, 2014; Pekny et al., 2014; Sofroniew, 2015). While glial fibrillary acidic protein (GFAP) and/or vimentin depletion as well as metabolic astrocyte inhibitors have been used to modulate the neural tissue after central nervous system injury, their efficacy in promoting functional recovery is still a matter of controversy (Ribotta et al., 2004; Hayakawa et al., 2010). Moreover, while GFAP is not homogeneously expressed in a normal post-matured CNS, it labels most astrocytes responding to an injury (Yasuda et al., 2004; Yang and Wang, 2015). Likewise, a study from Brozzi et al., (Brozzi et al., 2009) has shown that S100 calcium-binding protein B (S100B) is critical for glial cell migration and shaping. Indeed, S100B is also a commonly used biomarker after SCI (Yasuda et al., 2004; Oyinbo, 2011). It is then possible to hypothesize that the GFAP and S100B proteins levels (both classical markers of astrocytic reactivity and damage) might influence global levels of H4 acetylation, which constitutes an important insight into neural repair and tissue recovery after SCI.

The proposed study sought: a) to compare the global histone H4 acetylation levels at different time-points after a thoracic SCI model in rats; and b) to assess the relationship between GFAP/S100B markers post-SCI and the global histone H4 acetylation levels, since the former might influence the epigenetic machinery in injured rat spinal cord.

Materials and Methods
Animals
A total of 61 male Wistar rats (3 months old, body weight ~300 g) were obtained from the Central Animal House of the Institute of Basic Health Sciences, Federal University of Rio Grande do Sul, Brazil ($n = 18$ animals were used in experiment 1 and $n = 43$ in experiment 2). The animals were housed in standard laboratory conditions, with free access to food and water, under a 12-h light/dark cycle (lights on at 7:00 a.m.) with room temperature maintained at 22–24°C.

All procedures were in accordance with the National Institute of Health's Guide for the Care and Use of Laboratory Animals and with the Brazilian Council for Animal Experiments Control (Concea). The Animal Bioethics Committees of both the Universidade Federal do Rio Grande do Sul (process number 26116) and the Pontifícia Universidade Católica do Rio Grande do Sul (process number 15/00492) approved the study protocol.

Experimental design
In experiment 1 of the experiment, a morphological assay was performed. This was an important first step to guarantee that the SCI was detectable at the studied time points. Thus, the following groups were established: sham ($n = 3$); 6 hours post-SCI ($n = 3$); 24 hours post-SCI ($n = 3$); 48 hours post-SCI ($n = 3$); 72 hours post-SCI ($n = 3$); 7 days post-SCI ($n = 3$).

In experiment 2, the global H4 acetylation, GFAP and S100B levels were assessed in the spinal cord perilesional tissue. Moreover, we tested their possible association at the same above-mentioned time points. As above, the rats were divided into the sham ($n = 8$); 6 hours post-SCI ($n = 7$); 24 hours post-SCI ($n = 7$); 48 hours post-SCI ($n = 7$); 72 hours post-SCI ($n = 8$) and 7 days post-SCI ($n = 6$) groups.

Spinal cord injury model
Firstly, all animals were deeply anesthetized intraperitoneally with a mixture of xylasine (100–150 mg/kg) and ketamine (60–90 mg/kg). After that, the vertebral column was exposed between T9 and T10 and a total laminectomy was performed at T10 level without dura mater dissection. The New York University Impactor (NYU-Impactor®; W.M. Keck Center for Collaborative Neuroscience, USA) was used to induce a moderate SCI, as previously described (Nicola et al., 2016). Briefly, the exposed vertebral column was stabilized and the dorsal surface of the spinal cord received a 10-g weight dropped from a height of 25 mm. After the SCI procedure, animals were sutured in layers and housed in individual cages. Bladder evacuation was performed daily until they recovered the function. Enrofloxacin (Bayer, São Paulo, Brazil; 6 mg/kg) was administered for 7 days after the procedure to prevent secondary infection. The sham group received all the described procedures, with the exception of SCI induction.

Morphological assessment
In the first partof the experiment, rats were anesthetized with pentobarbital (100 mg/kg, i.p.; Cristália, Itapira, Brazil) and underwent transcardiac perfusion with 0.9% saline followed by 4% paraformaldehyde (Reagen, Colombo, Brazil) in 0.1 M phosphate buffer (PBS, pH 7.4) at each determined time-point after SCI. Following which, the spinal cord was removed (from C5 to L5), post-fixed in the same fixative solution and cryoprotected with 15% and 30% sucrose diluted in phosphate buffer saline (PBS). After that, the samples were frozen in isopentane, cooled in liquid nitrogen until slicing. For histological measurements, the thoracic region of the spinal cord was transversely cut into 20 μm sections

using a cryostat (Leica, Frankfurt, Germany) (Nicola et al., 2016). The sections were stained with hematoxylin and eosin technique and the images captured using a Nikon Eclipse E-600 microscope (Nikon Corporation, Tokyo, Japan) coupled to a digital camera. Thirty 20 µm cross-sections from each animal were used to analyze the cavitation area. Sequential sections with an interval of 300 µm were collected. The cavitation area in each sequential slice was determined and the largest cavitation area slice (called the epicenter) was identified. The epicenter was traced using ImageJ software (National Institutes of Health, Bethesda, MD, USA); any necrotic tissue within the cavities was considered part of the lesion and the total sum of the areas was calculated (Nicola et al., 2016).

ELISA assay
In the second part of the experiment, we performed the ELISA method to assess the global H4 acetylation, GFAP and S100B levels (Tramontina et al., 2007; de Mello et al., 2017). Rats were euthanized using a guillotine method, followed by spinal cord dissection. Spinal cord perilesional sections obtained from the T10 level (approximately 1 mm above or below) were randomly divided into two equal parts to process global H4 acetylation or GFAP and S100B levels.

Protein content
Lowry's method, with bovine-serum albumin (BSA) as standard, was used to determine the protein content (Tramontina et al., 2007).

Global H4 acetylation levels
Global H4 acetylation levels were measured using the Global Histone H4 Acetylation Assay Kit (Colorimetric Detection, catalog number P-4009, EpiQuik, Farmingdale, NY, USA) following the manufacturer's recommendation (capture antibody, 100 µg/mL and detection antibody, 400 µg/mL). Perilesional tissue was homogenized with a specific lysis buffer kit (nuclear extraction phase), which facilitated histone extraction. The samples were incubated in trichloroacetic acid, hydrochloric acid and acetone. Five centrifugations were performed during the entire protocol. The pellet obtained in this process was used to establish the global H4 acetylation levels. Then, the samples were incubated in the developing solution. Finally, the stopping solution was added. All readings were made at 405 nm in a 96 well-plate reader (ThermoPlate, São Paulo, Brazil). Results are expressed as ng/mg (de Mello et al., 2017).

GFAP levels
Perilesional tissue was homogenized in PBS (50 mM NaCl, 18 mM Na_2HPO_4, 83 mM $NaH_2PO_4·H_2O$, pH 7.4), containing 1 mM EGTA and 1mM phenylmethyl-sulphonyl fluoride. The GFAP content was measured using the ELISA method, as described (Tramontina et al., 2007; Leite et al., 2008). The GFAP assay consisted of coating the samples with 100 µL containing 70 µg of protein and leaving them overnight at 4°C. The next day, the samples were incubated in a polyclonal

anti-GFAP antibody from rabbit (2.9 g/L; Dako, Carpinteria, CA, USA) for 2 hours and then in a peroxidase-conjugated secondary antibody (1:1000, Dako) for 1 hour at room temperature. The color reaction with o-phenylenediamine-dihydrochloride (OPD) was measured at 492 nm. The standard GFAP curve ranged from 0.1 to 10 ng/mL. Results are expressed as ng/mg (Tramontina et al., 2007).

S100B levels
To assess the S100B levels, the same homogenized tissue used for GFAP detection was employed, as previously described (Tramontina et al., 2007; Leite et al., 2008). Briefly, 50 µL of sample plus 50 µL of Tris buffer were incubated for 2 hours on a microtiter plate, coated 30 minutes previously with a monoclonal anti-S100B antibody (4 g/L; Dako). After which, a peroxidase-conjugated anti-rabbit antibody (1:5000, Dako) was added for a further 30 minutes. The color reaction with OPD was measured at 492 nm. The standard S100B curve ranged from 0.02 to 1 ng/mL. Results are expressed as ng/µg of protein (Leite et al., 2008).

Statistical analysis
Data normality was assessed using the Shapiro-Wilk test. One-way analysis of variance followed by the Bonferroni *post hoc* test was used to detect group differences, as indicated. The relationship between astrocytic reactivity (levels of GFAP and S100B markers) and global H4 acetylation levels in the perilesional tissue was evaluated using Pearson's correlation coefficient test. All variables are expressed as mean ± standard error of the mean (SEM). Results were considered significant when $P \leq 0.05$. SPSS 17.0 (Statistical Package for the Social Sciences, Inc., Chicago, IL, USA) was used for the data analysis.

Results
There were no deaths or surgical complications (*i.e.*, wound infection) in this study. All spinal cord injured rats exhibited visible hindlimb motor deficits from immediate post-surgery to the end of the experiments. All evaluated outcomes exhibited normal distribution and, thus, parametric analyses were performed.

Cavitation area
The SCI model induced changes in the epicenter of the cystic cavity at the evaluated time-points ($F_{(5,17)} = 15.49$, $P = 0.0001$). Between-group (time-points) analysis revealed no changes between the sham and 6 hours post-SCI groups ($P = 0.97$). However, these same groups were different from the others: 24, 48, 72 hours and 7 days post-SCI groups ($P < 0.05$) (**Figure 1**). No additional differences were found. Together, these data suggest: a) the injury model was able to induce an experimental SCI in rats; and b) the cavity area at the lesion epicenter is comparable between the 24, 48, 72 hours and 7 days post-SCI groups. All these results are in agreement with the previous studies (Lv et al., 2011; Finelli et al., 2013; Chu et al., 2015; Nicola et al., 2016) and supported the second part of the study.
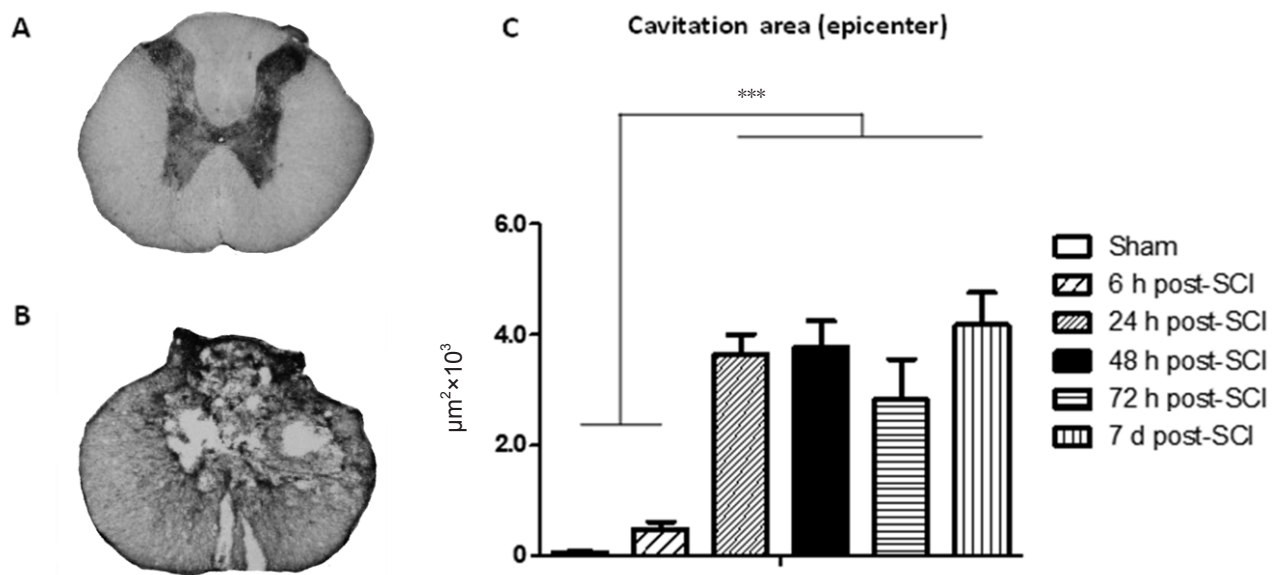
Figure 1 Cavitation area in the spinal cord injury (SCI) model.
(A) Sham spinal cord section in rats at thoracic level. (B) Histological image showing a spinal cord injury at T10 level. (C) Cavitation area in the lesion epicenter ($n = 18$). ***$P < 0.001$ (one-way analysis of variance followed by the Bonferroni *post hoc* test).
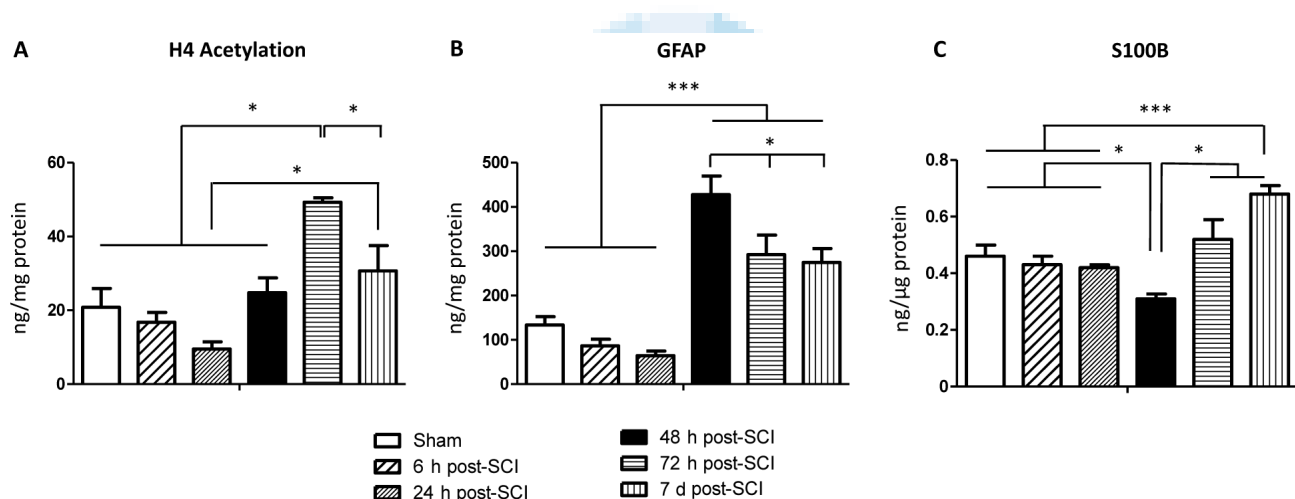
Figure 2 Global H4 acetylation, glial fibrillary acidic protein and S100 calcium-binding protein B levels at different time points after spinal cord injury (SCI).
(A) Global histone H4 acetylation; (B) glial fibrillary acidic protein (GFAP); and (C) S100 calcium-binding protein B (S100B) levels at studied time points. Data are expressed as the mean ± standard error of the mean (SEM) ($n = 43$). *$P < 0.05$ and ***$P < 0.001$ (one-way analysis of variance followed by the Bonferroni *post hoc* test).

Global histone H4 acetylation levels

One-way analysis of variance revealed that global histone H4 acetylation levels changed in the evaluated time-groups ($F_{(5,42)} = 12.94$, $P = 0.0001$). *Post hoc* tests showed the 72 hours post-SCI group differed from the other groups ($P < 0.05$), revealing an important increase in global histone H4 acetylation levels at that time-point. Moreover, there was an additional difference between the 24 hours and 7 days post-SCI groups ($P = 0.01$). No further differences were found between the sham group versus the 6, 24, 48 hours and 7 days post-SCI groups ($P > 0.05$) (**Figure 2A**). Overall, these data suggest global histone H4 acetylation levels in the per-

ilesional tissue are time-related after SCI.

GFAP levels

GFAP levels changed at the evaluated time-points ($F_{(5,42)} = 21.46$, $P = 0.0001$). Between-group analysis revealed the 48 hours post-SCI group differed from the other groups ($P < 0.05$). Moreover, the sham, 6 and 24 hours post-SCI groups were significantly different from the 72 hours and 7 days post-SCI groups ($P < 0.05$). No additional differences were found (**Figure 2B**). These results reinforce that GFAP is highly detectable 48 hours following SCI (considering the assessed endpoints).

Table 1 Relationship between global H4 acetylation versus GFAP and S100B protein levels at different time points

Group	GFAP levels	S100B levels
Sham	0.77 (0.02)*	–0.52 (0.18)
6 h post-SCI	–0.15 (0.74)	–0.35 (0.44)
24 h post-SCI	0.10 (0.86)	0.28 (0.95)
48 h post-SCI	–0.39 (0.93)	–0.09 (0.93)
72 h post-SCI	–0.54 (0.16)	–0.14 (0.72)
7 d post-SCI	0.10 (0.84)	–0.27 (0.10)
Pooled groups	0.44 (0.003)*	0.20 (0.19)
Pooled SCI groups	0.41 (0.01)*	0.31 (0.07)

Data are expressed as *r* value (*P* value). H4: Histone 4; GFAP: Glial fibrillary acidic protein; S100B: S100 calcium-binding protein B; r: Pearson's coefficient value; *P*: calculated probability; *Statistically significant difference.

S100B levels

Data analysis showed changes in S100B levels at the studied time-points ($F_{(5,42)}$=6.76, $P = 0.0001$). Interestingly, we observed the 48 hours post-SCI group had lower levels of S100B protein compared to the other studied time-point groups ($P < 0.03$). In addition, a significant increase in S100B levels was observed in the 7 days post-SCI group compared to the sham ($P = 0.02$), 6 hours ($P = 0.01$), 24 hours ($P = 0.006$) and 48 hours ($P = 0.001$) post-SCI groups (**Figure 2C**). These findings indicate that S100B and GFAP levels display different biochemical patterns (see above data) after SCI.

Relationship between astrocytic reactivity and global histone H4 acetylation levels

The relationship between both GFAP and S100B markers and global histone H4 acetylation levels are shown in **Table 1**. Because the levels of these proteins were time-related, the Pearson's correlation coefficient was run additionally in each studied time-group. There was a strong positive correlation between GFAP and global histone H4 acetylation levels only in the undamaged animals (sham group) ($r = 0.77$, $P = 0.02$). Additionally, there were significant correlations between GFAP and global H4 acetylation levels in pooled ($r = 0.44$, $P = 0.003$) and SCI-only ($r = 0.41$, $P = 0.01$) groups (**Table 1**). Moreover, no further correlations were observed between S100B and global H4 acetylation levels.

Discussion

The aims of this study were: a) to compare the global histone H4 acetylation levels at different time-points after a thoracic SCI model in rats; and b) to explore the relationship between two classical damage-related markers (GFAP and S100B) and the global histone H4 acetylation levels post-SCI. We hypothesize changes in global histone H4 acetylation levels could be time-related, which might lead to the identification of potential therapeutic windows for further epigenetic studies. Moreover, since GFAP has a pivotal role in modulating tissue plasticity after SCI (Chadi et al., 2001; Ribotta et al., 2004; Pekny et al., 2014), we assume the former could be associated with changes in global histone H4 acetylation

levels (Kurdistani et al., 2004). Overall, the current findings support the hypotheses. Results indicate global histone H4 acetylation levels exhibit a complex pattern after SCI, encompassing at least three clearly defined phases: no changes at 6, 24 and 48 hours post-SCI (first phase); increased levels at 72 hours post-SCI (second phase); and levels similar to controls in the 7 days post-SCI (third phase). These findings provide a new rational basis for further trials focusing on epigenetic interventions after SCI. Additionally, there were significant correlations between GFAP and global H4 acetylation levels.

This is the first study to show a thoracic SCI model can modulate the global H4 acetylation levels in a time-related way in which five different time-points were assessed during the first week following SCI. Thus, opportunities for like-for-like comparisons with other studies are limited. However, there are similarities with results obtained by previous studies investigating other aspects of epigenetic modulation and neuroplasticity. Global H4 acetylation levels were time-related after SCI, which was unsurprising since the former have been shown to vary in response to other stimuli in the CNS (Elsner et al., 2011; Lovatel et al., 2013; de Mello et al., 2017). Furthermore, increased H4 acetylation levels have been associated with learning, memory and brain plasticity (Elsner et al., 2011; Lovatel et al., 2013).

In this context, Finelli et al. (2013) reported increased levels of global histone H4 acetylation in dorsal root ganglion neurons after peripheral axotomy. A histone H4 hyperacetylated status induced by an HDAC inhibitor was shown to contribute to spinal cord plasticity and improve the potential for axonal growth and expression of regeneration-associated genes. After a conditioning lesion, the authors observed a 3-day peak of Smad1 expression, which has been described as an important cellular signal to activate sensory axon outgrowth mechanisms.

Notably, the histone acetylation-deacetylation balance modulates different cell types, such as inflammatory and immunological cells, which influence the severity of blood-brain barrier dysfunction, axonal demyelination, oxidative stress and injury impact (Faraco et al., 2006, 2009; Chuang et al., 2009). The present results could be understood in the same way, since the moments of increased global H4 acetylation levels might constitute a potential time-window to maximize repair of the remaining tissue. Thus, defining the epigenetic mechanisms linked to remodeling neural tissue would help researchers to design therapeutic strategies to promote wound healing and tissue functionality after spinal cord injury (Finelli et al., 2013; Wong and Zou, 2014).

There is a significant body of evidence suggesting histones and histone-modifying enzymes are able to reshape the chromatin structure and change the gene expression after CNS injury (Finelli et al., 2013; Kim et al., 2016; Wong and Zou, 2014). Several studies have suggested that HDACs and histone acetyltransferases play a central role in regulating histone proteins that impact on neuron and astrocyte gene expression (Hamby and Sofroniew, 2010; Majumder et al., 2013; Chu et al., 2015). Whilst global histone acetylation

profiles are less precise in determining gene expression than specific acetylation and deacetylation sites of lysine residues (located in the N termini of histones), it might be useful to globally monitor certain acetylation patterns in highly complex biological processes (Kurdistani et al., 2004), such as remodeling neural tissue after SCI.

Conversely, Lv et al. (2011) showed a sustained decrease of the histone H4 acetylation at one day, three day and one week post-SCI. This partial divergence in relation to the current results might be explained by several differences between the experiments. Firstly, the above-mentioned authors only used female rats in their experiments, which may influence the histone-acetylation profile, as previously suggested (Benoit et al., 2015). Secondly, variation in histone acetylation levels might be linked to between-study differences in sensorimotor spontaneous recovery (Finelli et al., 2013). Likewise, global histone H4 acetylation levels might differ according to the features of the analyzed tissue, such as injury severity, distance from the injury core and amount of damaged tissue in the collected samples (Kim et al., 2016). For instance, only perilesional tissue (1 mm above and below the T10 level of the spinal cord) was used in the current study. By contrast, Lv et al. (2011), did not indicate from at which levels of the spinal cord the samples were obtained. In addition, other common points of divergence between epigenetic studies are usually related to the species used (Viola and Loss, 2014), animal age (Dagnas and Mons, 2013), and variations in the experimental model (Finelli et al., 2013; Wong and Zou, 2014).

Interestingly, Kim et al. (2016) assessed the expression of the main regulators of cell survival and death using whole brain samples after a thoracic model of spinal cord injury in mice. They showed HDAC subtype 1 expression was increased in the brain at one week after the SCI, but not at three days or two weeks post-injury. Moreover, brain-derived neurotrophic factor and glial-derived neurotrophic factor were also up-regulated in the brain. These results, together with the findings of the present investigation, suggest SCI might modulate the epigenetic machinery depending on the assessed nervous system structure and the tissue context. Thus, the SCI may influence neural tissue not just in the perilesional area beyond the damaged spinal cord (Nicola et al., 2016).

From another perspective, treadmill exercise (Elsner et al., 2011; Lovatel et al., 2013; Spindler et al., 2014) and pharmacological interventions, such as valproic acid administration (Lv et al., 2011), can influence global histone H4 acetylation levels. Nonetheless, it is still unknown whether these interventions strengthen the relationship between histone H4 acetylation status and the expression of remodeling-related proteins in the damaged neural tissue. In addition, other epigenetic mechanisms, such as DNA methylation, acetylation of other histones, or lysine-specific acetylation in histone tails (Kurdistani et al., 2004; Saha and Pahan, 2006; Pelzel et al., 2010; Arrowsmith et al., 2012; Maleszkam, 2016), might influence cellular mechanisms in remodeling neural tissue. All these interesting basic research-derived issues are topics for further investigation.

The results also suggest GFAP and global H4 acetylation levels exhibit a positive correlation after SCI. Beyond the debate in the literature linking GFAP expression and histone acetylation (Chadi et al., 2001; Bailey et al., 2016), a previous study has suggested histone acetylation levels are associated with specific regulation of inflammatory genes (Tsaprouni et al., 2011). Thus, astrocyte reactivity might influence histone acetylation according to the features of the tissue microenvironment, which is also a matter for further study. In addition, we should be aware the current measurements were obtained from spinal cord parenchyma. Hence, whether GFAP expression changes global H4 acetylation at the cellular level, *i.e.*, according to astrocyte subtype, is still unknown, and is a research question beyond the scope of the present study.

The experiment also revealed the global histone H4 acetylation levels did not correlate with S100B levels in the spinal cord parenchyma. S100B is involved in several cellular mechanisms, such as extension control, shaping the astrocyte processes and glial scar progression (Yasuda et al., 2004). During astrocyte maturation, S100B is typically expressed later than GFAP (Brozzi et al., 2009; Bailey et al., 2016). Also, during reactive gliosis, S100B expression differs from that of GFAP (Burda et al., 2014). These factors may explain the current findings. Moreover, the onset of S100B expression is linked to a critical period in which GFAP-expressing cells achieve a stable stage and lose their neural stem cell potential (Raponi et al., 2007). Additionally, epigenetic factors might modulate S100B levels, which are still matter of debate (Nesic et al., 2005; Chelyshev et al., 2014).

GFAP and S100B are typically mentioned as astrocyte markers. However, Schwann cells also express both proteins at specific stages, particularly immature and non-myelinating Schwann cells. For example, Schwann cells infiltrate the lesion site following SCI (Church et al., 2017). Consequently, these cells may act at different time-points and influence GFAP and S100B expression and global H4 acetylation levels. Further research is needed to clarify this issue.

This study has some limitations. Whilst many cell types within the perilesional tissue may influence GFAP, S100B and global H4 acetylation expression, assessing the full tissue sample is more feasible for clinical translation. For example, during the spinal cord surgery time is usually unavailable for typical immunohistochemical processing and detailed data analyses. Thus, the source of the marker might be of secondary importance if the levels of a biochemical compound in the tissue can be used as a biomarker. Identifying which cells (astrocytes, microglia, Schwann cells, neurons or others) provoke altered GFAP, S100B or global H4 acetylation levels after SCI is an issue for further studies. In addition, HDAC inhibitors would help clarify the hypothesized relationship between global H4 acetylation, GFAP and S100B levels in functional recovery.

In summary, this study presents an attempt to bridge the gap between SCI-induced epigenetic changes in rats.

Indeed, we showed global histone H4 acetylation levels in spinal cord parenchyma are time-related, providing basic knowledge for further epigenetic interventions. In addition, we also suggest GFAP is associated to the global histone H4 acetylation levels in remodeling spinal cord parenchyma. Finally, further studies using other epigenetic biomarkers are needed to clarify their influence on repair of remaining tissue after SCI.

References

Abeysinghe HC, Phillips EL, Chin-Cheng H, Beart PM, Roulston CL (2016) Modulating astrocyte transition after stroke to promote brain rescue and functional recovery: emerging targets include Rho kinase. Int J Mol Sci 17:288.

Arrowsmith CH, Bountra C, Fish PV, Lee K, Schapira M (2012) Epigenetic protein families: a new frontier for drug discovery. Nat Rev Drug Discov 11:384-400.

Bailey ZS, Grinter MB, VandeVord PJ (2016) Astrocyte reactivity following blast exposure involves aberrant histone acetylation. Front Mol Neurosci 9:64.

Benoit JD, Rakic P, Frick KM (2015) Prenatal stress induces spatial memory deficits and epigenetic changes in the hippocampus indicative of heterochromatin formation and reduced gene expression. Behav Brain Res 281:1-8.

Brozzi F, Arcuri C, Giambanco I, Donato R (2009) S100B protein regulates astrocyte shape and migration via interaction with Src kinase: implications for astrocyte development, activation, and tumor growth. J Biol Chem 284:8797-8811.

Burda JE, Sofroniew MV (2014) Reactive gliosis and the multicellular response to CNS damage and disease. Neuron 81:229-248.

Chadi G, Andrade MS, Leme RJ, Gomide VC (2001) Experimental models of partial lesion of rat spinal cord to investigate neurodegeneration, glial activation, and behavior impairments. Int J Neurosci 111:137-165.

Chelyshev YA, Muhamedshina YO, Povysheva TV, Shaymardanova GF, Rizvanov AA, Nigmetzyanova MV, Tiapkina OV, Bondarenko NI, Nikolskiy EE, Islamov RR (2014) Characterization of spinal cord glial cells in a model of hindlimb unloading in mice. Neuroscience 280:328-339.

Chu W, Yuan J, Huang L, Xiang X, Zhu H, Chen F, Chen Y, Lin J, Feng H (2015) Valproic Acid Arrests Proliferation but Promotes Neuronal Differentiation of Adult Spinal NSPCs from SCI Rats. Neurochem Res 40:1472-1486.

Chuang DM, Leng Y, Marinova Z, Kim HJ, Chiu CT (2009) Multiple roles of HDAC inhibition in neurodegenerative conditions. Trends Neurosci 32:591-601.

Church JS, Milich LM, Lerch JK, Popovich PG, McTigue DM (2017) E6020, a synthetic TLR4 agonist, accelerates myelin debris clearance, Schwann cell infiltration, and remyelination in the rat spinal cord. Glia 65:883-899.

Dagnas M, Mons N (2013) Region- and age-specific patterns of histone acetylation related to spatial and cued learning in the water maze. Hippocampus 23:581-591.

de Mello AS, da Silva IR, Reinaldo GP, Dorneles GP, Ce J, Lago PD, Peres A, Elsner VR, Coelho JC (2017) The modulation of inflammatory parameters, Brain-derived neurotrophic factor levels and global histone H4 acetylation status in peripheral blood of patients with Gaucher disease type 1. Clin Biochem 50:228-233.

Di Giammartino DC, Apostolou E (2016) The chromatin signature of pluripotency: establishment and maintenance. Curr Stem Cell Rep 2:255-262.

Elsner VR, Lovatel GA, Bertoldi K, Vanzella C, Santos FM, Spindler C, de Almeida EF, Nardin P, Siqueira IR (2011) Effect of different exercise protocols on histone acetyltransferases and histone deacetylases activities in rat hippocampus. Neuroscience 192:580-587.

Faraco G, Pancani T, Formentini L, Mascagni P, Fossati G, Leoni F, Moroni F, Chiarugi A (2006) Pharmacological inhibition of histone deacetylases by suberoylanilide hydroxamic acid specifically alters gene expression and reduces ischemic injury in the mouse brain. Mol Pharmacol 70:1876-1884.

Faraco G, Pittelli M, Cavone L, Fossati S, Porcu M, Mascagni P, Fossati F, Moroni F, Chiarugi A (2009) Histone deacetylase (HDAC) inhibitors reduce the glial inflammatory response in vitro and in vivo. Neurobiol Dis 36:269-279.

Finelli MJ, Wong JK, Zou H (2013) Epigenetic regulation of sensory axon regeneration after spinal cord injury. J Neurosci 33:19664-19676.

Hamby ME, Sofroniew MV (2010) Reactive astrocytes as therapeutic targets for CNS disorders. Neurotherapeutics 7:494-506.

Hayakawa K, Nakano T, Irie K, Higuchi S, Fujioka M, Orito K, Iwasaki K, Jin G, Lo EH, Mishima K, Fujiwara M (2010) Inhibition of reactive astrocytes with fluorocitrate retards neurovascular remodeling and recovery after focal cerebral ischemia in mice. J Cereb Blood Flow Metab 30:871-882.

Herman D, Jenssen K, Burnett R, Soragni E, Perlman SL, Gottesfeld JM (2006) Histone deacetylase inhibitors reverse gene silencing in Friedreich's ataxia. Nat Chem Biol 2:551-558.

Jin H, Kanthasamy A, Harischandra DS, Kondru N, Ghosh A, Panicker N, Anantharam V, Rana A, Kanthasamy AG (2014) Histone hyperacetylation up-regulates protein kinase Cdelta in dopaminergic neurons to induce cell death: relevance to epigenetic mechanisms of neurodegeneration in Parkinson disease. J Biol Chem 289:34743-34767.

Kim JH, Kim SH, Cho SR, Lee JY, Baek A, Jung HS (2016) The modulation of neurotrophin and epigenetic regulators: implication for astrocyte proliferation and neuronal cell apoptosis after spinal cord injury. Ann Rehabil Med 40:559-567.

Kim MS, Akhtar MW, Adachi M, Mahgoub M, Bassel-Duby R, Kavalali ET, Olson EN, Monteggia LM (2012) An essential role for histone deacetylase 4 in synaptic plasticity and memory formation. J Neurosci 32:10879-10886.

Kurdistani SK, Tavazoie S, Grunstein M (2004) Mapping global histone acetylation patterns to gene expression. Cell 117:721-733.

Lee BB, Cripps RA, Fitzharris M, Wing PC (2011) The global map for traumatic spinal cord injury epidemiology: update 2011, global incidence rate. Spinal Cord 52:110-116.

Leite MC, Galland F, Brolese G, Guerra MC, Bortolotto JW, Freitas R, Almeida LM, Gottfried C, Goncalves CA (2008) A simple, sensitive and widely applicable ELISA for S100B: Methodological features of the measurement of this glial protein. J Neurosci Methods 169:93-99.

Lovatel GA, Elsner VR, Bertoldi K, Vanzella C, Moyses Fdos S, Vizuete A, Spindler C, Cechinel LR, Netto CA, Muotri AR, Siqueira IR (2013) Treadmill exercise induces age-related changes in aversive memory, neuroinflammatory and epigenetic processes in the rat hippocampus. Neurobiol Learn Mem 101:94-102.

Lv L, Sun Y, Han X, Xu CC, Tang YP, Dong Q (2011) Valproic acid improves outcome after rodent spinal cord injury: potential roles of histone deacetylase inhibition. Brain Res 1396:60-68.

Majumder A, Dhara SK, Swetenburg R, Mithani M, Cao K, Medrzycki M, Fan Y, Stice SL (2013) Inhibition of DNA methyltransferases and histone deacetylases induces astrocytic differentiation of neural progenitors. Stem Cell Res 11:574-586.

Maki T, Hayakawa K, Pham LD, Xing C, Lo EH, Arai K (2013) Biphasic mechanisms of neurovascular unit injury and protection in CNS diseases. CNS Neurol Disord Drug Targets 12:302-315.

Maleszka R (2016) Epigenetic code and insect behavioural plasticity. Curr Opin Insect Sci 15:45-52.

Nesic O, Lee J, Johnson KM, Ye Z, Xu GY, Unabia GC, Wood TG, McAdoo DJ, Westlund KN, Hulsebosch CE, Regino Perez-Polo J (2005) Transcriptional profiling of spinal cord injury-induced central neuropathic pain. J Neurochem 95:998-1014.

Nicola FC, Rodrigues LP, Crestani T, Quintiliano K, Sanches EF, Willborn S, Aristimunha D, Boisserand L, Pranke P, Netto CA (2016) Human dental pulp stem cells transplantation combined with treadmill training in rats after traumatic spinal cord injury. Braz J Med Biol Res 49:e5319.

Oyinbo CA (2011) Secondary injury mechanisms in traumatic spinal cord injury: a nugget of this multiply cascade. Acta Neurobiol Exp (Wars) 71:281-299.

Park M, Keung AJ, Khalil AS (2016) The epigenome: the next substrate for engineering. Genome Biol 17:183.

Pekny M, Pekna M (2014) Astrocyte reactivity and reactive astrogliosis: costs and benefits. Physiol Rev 94:1077-1098.

Pekny M, Wilhelmsson U, Pekna M (2014) The dual role of astrocyte activation and reactive gliosis. Neurosci Lett 565:30-38.

Pelzel HR, Schlamp CL, Nickells RW (2010) Histone H4 deacetylation plays a critical role in early gene silencing during neuronal apoptosis. BMC Neurosci 11:62.

Raponi E, Agenes F, Delphin C, Assard N, Baudier J, Legraverend C, et al (2007) S100B expression defines a state in which GFAP-expressing cells lose their neural stem cell potential and acquire a more mature developmental stage. Glia 15:165-177.

Ribotta MG, Menet V, Privat A (2004) Glial scar and axonal regeneration in the CNS: lessons from GFAP and vimentin transgenic mice. Acta Neurochir Suppl 89:87-92.

Saha RN, Pahan K (2006) HATs and HDACs in neurodegeneration: a tale of disconcerted acetylation homeostasis. Cell Death Differ 13:539-550.

Silva NA, Sousa N, Reis RL, Salgado AJ (2014) From basics to clinical: a comprehensive review on spinal cord injury. Prog Neurobiol 114:25-57.

Sofroniew MV (2015) Astrocyte barriers to neurotoxic inflammation. Nat Rev Neurosci 16:249-263.

Spindler C, Cechinel LR, Basso C, Moyses F, Bertoldi K, Roesler R, Lovatel GA, Rostirola Elsner V, Siqueira IR (2014) Treadmill exercise alters histone acetyltransferases and histone deacetylases activities in frontal cortices from wistar rats. Cell Mol Neurobiol 34:1097-1101.

Tasker RC, Duncan ED (2015) Focal cerebral ischemia and neurovascular protection: a bench-to-bedside update. Curr Opin Pediatr 27:694-699.

Tramontina F, Leite MC, Cereser K, de Souza DF, Tramontina AC, Nardin P, Andreazza AC, Gottfried C, Kapczinski F, Goncalves CA (2007) Immunoassay for glial fibrillary acidic protein: antigen recognition is affected by its phosphorylation state. J Neurosci Methods 162:282-286.

Tsaprouni LG, Ito K, Powell JJ, Adcock IM, Punchard N (2011) Differential patterns of histone acetylation in inflammatory bowel diseases. J Inflamm (Lond) 8:1.

Viola GG, Loss CM (2014) Letter to Editor about: "Physical exercise increases GFAP expression and induces morphological changes in hippocampal astrocytes". Brain Struct Funct 219:1509-1510.

Vogel-Ciernia A, Matheos DP, Barrett RM, Kramár EA, Azzawi S, Chen Y, Magnan CN, Zeller M, Sylvain A, Haettig J, Jia Y, Tran A, Dang R, Post RJ, Chabrier M, Babayan AH, Wu JI, Crabtree GR, Baldi P, Baram TZ, et al. (2013) The neuron-specific chromatin regulatory subunit BAF53b is necessary for synaptic plasticity and memory. Nat Neurosci 16:552-561.

Watson LA, Tsai LH (2017) In the loop: how chromatin topology links genome structure to function in mechanisms underlying learning and memory. Curr Opin Neurobiol 43:48-55.

Wong JK, Zou H (2014) Reshaping the chromatin landscape after spinal cord injury. Front Biol (Beijing) 9:356-366.

Wu KW, Kou ZW, Mo JL, Deng XX, Sun FY (2016) Neurovascular coupling protects neurons against hypoxic injury via inhibition of potassium currents by generation of nitric oxide in direct neuron and endothelium cocultures. Neuroscience 334:275-282.

Yang Z, Wang KK (2005) Glial fibrillary acidic protein: from intermediate filament assembly and gliosis to neurobiomarker. Trends Neurosci 38:364-374.

Yasuda Y, Tateishi N, Shimoda T, Satoh S, Ogitani E, Fujita S (2004) Relationship between S100beta and GFAP expression in astrocytes during infarction and glial scar formation after mild transient ischemia. Brain Res 1021:20-31.

Yu IT, Park JY, Kim SH, Lee JS, Kim YS, Son H (2009) Valproic acid promotes neuronal differentiation by induction of proneural factors in association with H4 acetylation. Neuropharmacology 56:473-480.